Table 1: Decoder latencies

Decoder width	Rising edge (ps)	Falling edge (ps)
3:8	150	100
4:16	230	100
5:32	300	100
6:64	400	100

Finally, an estimation of the latency associated to memories and decoder is required to verify that it does not turn to be a critical issue. In this case timing constraints are relaxed since these delays concern exclusively the initialisation phases when the system switches between two contexts. Table 1 shows latencies for different decoder widths, and it can be seen that, even if an area driven design methodology was followed, delays are short anyway.

Conclusion: A decoder-based interconnect structure has been presented that reduces the area overhead introduced by multi-context FPGAs with no penalty in routing delays with respect to a classic approach. Circuits of a multi-context memory and a new decoder have been illustrated in order to use the minimum number of transistors. Adopting the proposed approach a dramatic reduction in interconnection area can be achieved, up to 75% for an eight-context FPGA.

Acknowledgment: The authors would like to thank STMicroelectronics CR&D for funding and support.

22 November 2002
Electronics Letters Online No: 20030204
DOI: 10.1049/el:20030204

A. Lodi, L. Ciccarelli, A. Cappelli, F. Campi and M. Toma (*ARCES, Università di Bologna, Viale Risorgimento, 2, 40136 Bologna, Italy*)

E-mail: andrea.lodi@deis.unibo.it

References

1 MURPHY, C.W., and HARVEY, D.M.: 'Reconfigurable hardware implementation of BinDCT', *Electron. Lett.*, 2002, **38**, (18), pp. 1012–1013
2 DEHON, A.: 'DPGA-coupled microprocessors: commodity ICs for the early 21st century'. Proc. IEEE Symp. on FCCM, Napa Valley, CA, USA, April 1994, pp. 31–39
3 TRIMBERGER, S., CARBERRY, D., JHONSON, A., and WONG, J.: 'A time multiplexed FPGA'. Proc. IEEE Symp. on FCCM, Napa Valley, CA, USA, April 1997, pp. 34–40
4 BAENA-LECUYER, V., AGUIRRE, M., TORRALBA, A., FRANQUELO, L., and FAURA, J.: 'Decoder-driven switching matrices in multicontext fpgas: area reduction and their effect on routability'. Proc. IEEE ISCAS'99, Orlando, FL, USA, 1999, Vol. 1, pp. 463–466

High optical power electroabsorption waveguide modulator

L.A. Johansson, Y.A. Akulova, G.A. Fish and L.A. Coldren

A sampled grating distributed Bragg reflector-laser integrated with a waveguide Franz-Keldysh modulator is investigated for high optical power applications. The EAM modulation efficiency is demonstrated to asymptotically approach a limit determined by the internal differential photodetector efficiency. Linear photocurrent and 1 dB small signal AC compression point both exceed 70 mA, indicating high saturation power.

Introduction: High optical power tolerance of modulators is a key requirement for the design of low-loss, high-fidelity optical links. For low-loss analogue links, $LiNbO_3$ Mach-Zehnder modulators are commonly preferred to electroabsorption modulators (EAMs) because of the better power handling. Electroabsorption modulators have the advantages of generally lower driving voltage and ease of integration with a laser source, reducing optical losses and costs. Limitations to the available optical power in an EAM include carrier pile-up, particularly in multiple quantum well (MQW) modulators [1], and facet damage [2]. In this Letter, we investigate the prospect of using a sampled grating distributed Bragg reflector (SGDBR)-integrated Franz-Keldysh EAM as a modulator or photodetector for applications requiring high optical power, such as low-loss, high-fidelity analogue optical links.

Device: The investigated device is integrated on the same InP chip with an SGDBR laser and a semiconductor optical amplifier (SOA) [3]. The integration of the laser and SOA active regions with the tuning and modulator sections of the device has been accomplished by using an offset quantum-well structure [4]. In this simple integration technology the active region of the modulator uses the same bulk quaternary waveguide as the tuning sections of the laser. The Franz-Keldysh effect in the bulk waveguide material provides for larger spectral bandwidth compared to the quantum-confined Stark effect, as shown by Fig. 1. The bandwidth is RC-limited at 6.5 GHz. However, the FKE-bulk design allows improved power handling of the device, avoiding carrier pile-up problems. The power handling of the device is limited by Joule-heating to ~200 mW *I–V* product, *I* being the EAM photocurrent. Integration also allows efficient coupling of potentially very high waveguide optical power by avoiding modulator facet damage due to high power at the input fibre interface, shown to limit the input optical power to typically 200mW [2]. The efficient coupling between the source and the modulator makes it convenient to study high optical power effects in the device, but the modulator performance will not be possible to define in relation to input optical power and therefore have to be related to either the output optical power or detected photocurrent.

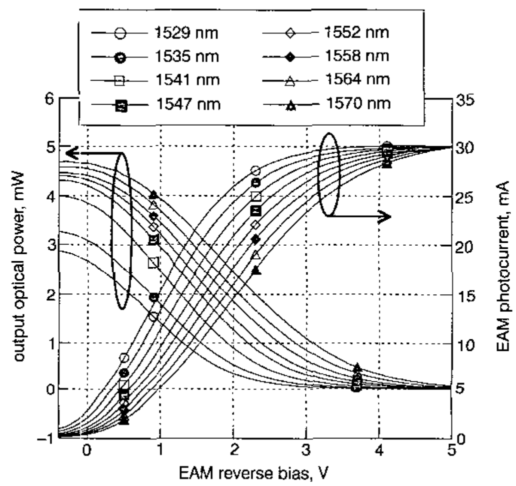

Fig. 1 *Measured output optical power and absorbed photocurrent of modulator against EAM reverse bias at different optical wavelengths*

Modulator performance: To analyse the signal current gain in an optical link, the responsivity of the optical transmitter and receiver can be expressed in terms of equivalent optical conversion efficiency, where 100% corresponds to 1.24 A/W and 0.81 W/A for receiver and transmitter, respectively, at 1550 nm. For a uniform and high modulator bandwidth, the EAM is terminated by an AC-coupled 50 Ω load, providing a current drain for the AC signal and reducing the effective responsivity of the modulator. At sufficiently high optical power, the detected photocurrent from the electroabsorption will degrade the modulator responsivity. The photocurrent can be modelled as an equivalent junction resistance, corresponding to the modulation current slope sensitivity dV/dI, over the EAM, corrected by a serial resistance, here estimated to 7 Ω [5]. Fig. 2 shows the equivalent junction resistance against average EAM photocurrent at the bias point of maximum slope sensitivity. The first curve is derived from DC data and the second curve is derived from the detected modulated signal current, also shown in Fig. 2, normalised to the 50 Ω external load at very low modulator photocurrent to compensate for RF and optical coupling losses. It is seen that the lower modulation sensitivity at high optical power can be well accounted for by the impact of the absorbed photocurrent. The increase of the slope sensitivity at high optical power remains small, only 7% higher at 30 mA photocurrent, indicating low thermal bandgap shrinkage. It is worth noting that at high optical power, the optical conversion efficiency is mainly limited by the photocurrent, rather than the 50 Ω load current drain. A minimum estimate of the waveguide modulation efficiency at 30 mA average photocurrent is 61%, using the assumption that the internal differential photodetection efficiency (η_d) is 100%. In fact, the internal modulation efficiency in an electroabsorption modulator will asymptotically approach $(\eta_d)^{-1}$ with increasing optical power. If the use of electroabsorption modulators for optical links with signal current gain will be viable, the photodetection efficiency of the modulator will need to be significantly reduced. The projected efficiency of this modulator, η_d being 0, would be at a minimum 156%. Further, the 200 mW I–V limit allows an increase of the input optical power, showing a promising prospect for the application of Franz-Keldysh modulators for optical links with RF gain.

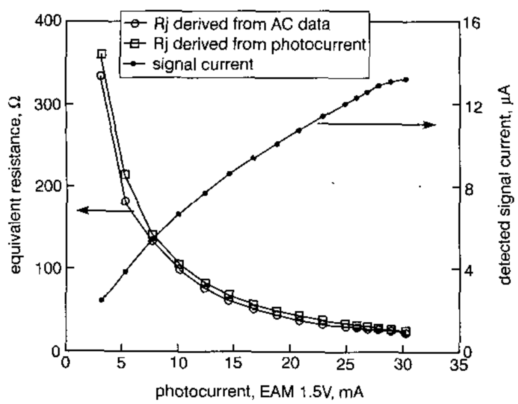

Fig. 2 *Device modulation sensitivity against average modulator DC photocurrent at maximum slope sensitivity*

Second curve obtained from DC data, first curve obtained from detected 6 GHz signal current, shown on left scale, normalised to 50 V/A at <1 mA photocurrent

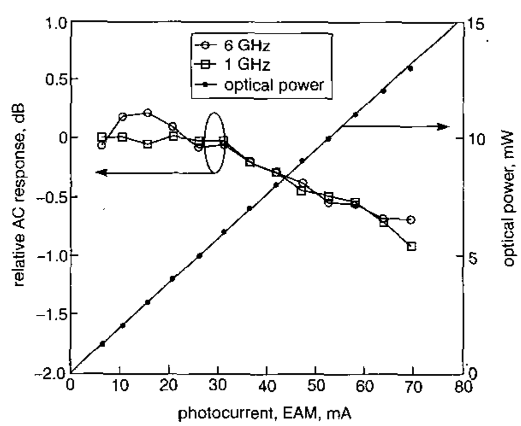

Fig. 3 *Left scale shows measured small signal AC response of waveguide detector against received photocurrent at 1558 nm; right scale shows DC photocurrent against optical output power at 1558 nm*

EAM biased at −2.8 V for detection and unbiased for transmission

The saturation power of the EAM, decoupled from the reduction of modulation sensitivity due to photocurrent, can be estimated from observations on the EAM photocurrent. Fig. 1 shows the transmitted optical power and detected EAM photocurrent against bias voltage for various wavelengths within the tuning range of the source. The optical input power is adjusted to 30 mA photocurrent at −5 V bias voltage, where the absorption approaches 100% for all wavelengths. The transmitted power decreases at lower wavelengths mainly due to passive waveguide loss. As seen in Fig. 1, the absorbed photocurrent is closely related to the transmission. Fig. 3 shows the photocurrent for an EAM bias voltage of −2.8 V, against transmitted optical power, the detector being unbiased. The detected photocurrent follows a nearly perfectly linear relation to the optical output power up to 70 mA of detected photocurrent. The small signal AC response is measured by modulating the gain section, and using the SOA bias current to regulate the received photocurrent. Fig. 3 shows the measured small signal AC response of the detector against received photocurrent. The uncertainty in the measurement at lower received photocurrents are due to crosstalk from the modulation signal as the gain section and modulator are located on the same chip. The AC response shows a small degradation at increasing photocurrents, however, the projected 1 dB compression point lies beyond 70 mA of received photocurrent. No significant difference in AC linearity is detected between 1 GHz and close to the modulation bandwidth, 6 GHz. This is confirmed by the bandwidth of the device, which lies independent of received photocurrent at 6.5 GHz.

Conclusion: We have investigated the prospect of using a Franz-Keldysh modulator or a detector for applications requiring high optical power, such as low-loss, high-fidelity analogue optical links. Operation over a large bandwidth, 1529 to 1570 nm, has been demonstrated. It is shown that integration of an electroabsorption modulator with the optical source is an elegant solution to allow the EAM to operate at power levels necessary to achieve signal gain by ensuring efficient coupling and not being susceptible to facet damage at high input optical power. The bulk design is also less sensitive to carrier pile-up effects than quantum-well based modulators, allowing the overall power level to be limited by Joule-heating. High saturation power is indicated by observations on the photocurrent linearity and the 1 dB small signal photodetection AC compression point, both exceeding 70 mA. For the prospect of signal gain to be realised, the photocurrent needs to be reduced. It is experimentally shown how the EAM modulation efficiency expressed in W/A will asymptotically approach a limit determined by the inverse of the internal differential photodetection efficiency. Here, eliminating the photocurrent would increase the equivalent modulation efficiency from 60 to 158% over the 50 Ω terminated device and allow higher waveguide power by reducing Joule-heating.

Acknowledgments: L.A. Johansson and L.A. Goldren wish to thank G. Fish and Y. Akulova at Agility Communications Inc. for supplying the device. This work was supported by the DARPA RFLICS program via SPAWAR.

19 December 2002

Electronics Letters Online No: 20030264

DOI: 10.1049/el:20030264

L.A. Johansson and L.A. Coldren (*Department of Electrical and Computer Engineering, University of California, Santa Barbara, CA 93106, USA*)

E-mail: leif@ece.ucsb.edu

Y.A. Akulova and G.A. Fish (*Agility Communications, Inc., 600 Pine Ave, Santa Barbara, CA 93117, USA*)

References

1 SHIN, D.S., CHEN, W.X., ZHUANG, Y., WU, Y., PAPPERT, S.A., CHOW, D., YAP, D., DEELMAN, P., and YU, P.K.L.: 'Suppressing electroabsorption with intra-step-barrier quantum wells for high-power electroabsorption modulators', *Electron. Lett.*, 2002, **38**, pp. 1140–1142

2 ISLAM, M.S., MURTHY, S., ITOH, T., WU, M.C., NOVAK, D., WATERHOUSE, R.B., SIVCO, D.L., and CHO, A.Y.: 'Velocity-matched distributed photodetectors and balanced photodetectors with p-i-n photodiodes', *IEEE Trans. Microw. Theory Tech.*, 2001, **49**, pp. 1914–1920

3 AKULOVA, Y.A., FISH, G.A., KOH, P.C., SCHOW, C., KOZODOY, P., DAHL, A., NAKAGAWA, S., LARSON, M., MACK, M., STRAND, T., COLDREN, C., HEGBLOM, E., PENNIMAN, S., WIPIEJEWSKI, T., and COLDREN, L.A.: 'Widely-tunable electroabsorption-modulated sampled grating DBR laser transmitter', *J. Sel. Top. Quantum Electron.*, (to be published)

4 MASON, B., FISH, G.A., DENBAARS, S.P., and COLDREN, L.A.: 'Widely tunable sampled grating DBR laser with integrated electroabsorption modulator', *IEEE Photonics Technol. Lett.*, 1999, **11**, pp. 638–640

5 LI, G.L., YU, P.K.L., CHANG, W.S.C., LOI, K.K., SUN, C.K., and PAPPERT, S.A.: 'Concise RF equivalent circuit model for electroabsorption modulators', *Electron. Lett.*, 2000, **36**, pp. 818–820